Bayesian Modeling of Quantum-Dot-Cellular-Automata Circuits

Sanjukta Bhanja, Saket Srivastava

Department of Electrical Engineering
University of South Florida, Tampa, USA
(bhanja, ssrivast)@eng.usf.edu

ABSTRACT

The goal of this work is to develop a fast, Bayesian Probabilistic Computing model [1], [2] that exploits the induced causality of clocking to arrive at a model with the minimum possible complexity. The probabilities directly model the quantum-mechanical steady-state probabilities (density matrix) or equivalently, the cell polarizations. The attractive feature of this model is that not only does it model the strong dependencies among the cells, but it can be used to compute the steady state cell polarizations, without iterations or the need for temporal simulation of quantum mechanical equations. The impact of our proposed modeling is that it is based on density matrix-based quantum modeling, takes into account dependency patterns induced by clocking, and is non-iterative. It allows for quick estimation and comparison of quantum-mechanical quantities for a QCA circuit, such as QCA-state occupancy probabilities or polarizations at any cell, thus enable one to quickly compare, contrast, and fine tune clocked QCA circuit designs, before performing costly full quantum-mechanical simulation of the temporal dynamics.

Keywords: quantum-dot cellular automata, bayesian networks, probabilistic computing, qca computing

1 Introduction

Quantum-dot Cellular Automata (QCA) is an emerging technology that offer a revolutionary approach to computing at nano-level [3]. It tries to exploit, rather than treat as nuisance properties, the inevitable nano-level issues, such as device to device interaction, to perform computing. Other advantages include the lack of interconnects, potential for implementation in metal [3], and using molecules [4]. Molecular implementation has potential for room temperature operations.

The **goal** of this work is to develop a fast, Bayesian Probabilistic Computing model [1], [2] that exploits the induced causality of clocking to arrive at a model with the minimum possible complexity. The probabilities directly model the quantum-mechanical steady-state probabilities (density matrix) or equivalently, the cell polarizations. The attractive feature of this model is that not only does it model the strong dependencies among the cells, but it can be used to compute the steady state cell polarizations, without iterations or the need for temporal simulation of quantum mechanical equations.

The **impact** of our proposed modeling is that it is based on density matrix-based quantum modeling, takes into account dependency patterns induced by clocking, and is non-iterative. It allows for quick estimation and comparison of quantum-mechanical quantities for a QCA circuit, such as QCA-state occupancy probabilities or polarizations at any cell, their dependence on temperature, or any parameter that depends on them. This will enable one to quickly compare, contrast and fine tune clocked QCA circuits designs, before performing costly full quantum-mechanical simulation of the temporal dynamics.

We validate our modeling with coherence vector based temporal simulation for various QCA systems (Fig. 5). We also show, using the *clocked* majority gate, how the model can used to study dependencies with respect to temperature and inputs (Fig. 5).

2 Prior Work

Previous work in modeling QCA circuits include the bistable simulation engine and the nonlinear approximation [5]–[7], however, these methods are iterative and do not produce steady state polarization estimates. In other words, they estimate just state assignments and not the probabilities of being in these states. The coherence vector based method [8], [7] does explicitly estimate the polarizations, but it is appropriate when one needs full temporal dynamics simulation (Bloch equation), and hence is extremely slow; for a full adder design with about 150 cells it takes about 500 seconds for 8 input vectors. Perhaps, the only approach that can estimate polarization for QCA cells, without full quantum-mechanical simulation is the thermodynamic model proposed in [9], but it is based on semi-classical Ising approximation.

Following Tougaw and Lent [10] and other subsequent works on QCA, we use the two-state approximate model of a single QCA cell. We denote the two possible, orthogonal, eigenstates of a cell by $|1\rangle$ and $|0\rangle$. The state at time t, which is referred to as the wave-function and denoted by $|\Psi(t)\rangle$, is a linear combination of these two states, i.e. $|\Psi(t)\rangle = c_1(t)|1\rangle + c_2(t)|0\rangle$. Note that the coefficients are function of time. The expected value of any observable, $\langle\hat{A}(t)\rangle$, can be expressed in terms of the wave function as $\langle\hat{A}\rangle = \langle\Psi(t)|\hat{A}(t)|\Psi(t)\rangle$ or equivalently as $\mathrm{Tr}[\hat{A}(t)|\Psi\rangle(t)\langle\Psi(t)|]$,

where Tr denotes the trace operation, $\mathrm{Tr}[\cdots] = \langle 1|\cdots|1\rangle + \langle 0|\cdots|0\rangle$. The term $|\Psi(t)\rangle\langle\Psi(t)|$ is known as the density operator, $\hat{\rho}(t)$. Expected value of any observable of a quantum system can be computed if $\hat{\rho}(t)$ is known.

A 2 by 2 matrix representation of the density operator, in which entries denoted by $\rho_{ij}(t)$ can be arrived at by considering the projections on the two eigenstates of the cell, i.e. $\rho_{ij}(t) = \langle i|\hat{\rho}(t)|j\rangle$. This can be simplified further.

$$\begin{aligned} \rho_{ij}(t) &= \langle i|\hat{\rho}(t)|j\rangle \\ &= \langle i|\Psi(t)\rangle\langle\Psi(t)|j\rangle = (\langle i|\Psi(t)\rangle)(\langle j|\Psi(t)\rangle)^* \\ &= c_i(t)c_j^*(t) \end{aligned} \tag{1}$$

The density operator is a function of time and using Loiuville equations we can capture the temporal evaluation of $\rho(t)$ in Eq. 2.

$$\hbar\frac{\partial}{\partial t}\rho(\mathbf{t}) = \mathbf{H}\rho(\mathbf{t}) - \rho(\mathbf{t})\mathbf{H} \tag{2}$$

where H is a 2 by 2 matrix representing the Hamiltonian of the cell and using Hartree approximation. Expression of Hamiltonian is shown in Eq. 3 [10].

$$\mathbf{H} = \begin{bmatrix} -\frac{1}{2}\sum_i E_k P_i f_i & -\gamma \\ -\gamma & \frac{1}{2}\sum_i E_k P_i f_i \end{bmatrix} = \begin{bmatrix} -\frac{1}{2}E_k\bar{P} & -\gamma \\ -\gamma & \frac{1}{2}E_k\bar{P} \end{bmatrix} \tag{3}$$

where the sums are over the cells in the local neighborhood. E_k is the "kink energy" or the energy cost of two neighboring cells having opposite polarizations. f_i is the geometric factor capturing electrostatic fall off with distance between cells. P_i is the polarization of the i-th cell. And, γ is the tunneling energy between two cell states, which is controlled by the clocking mechanism. The notation can be further simplified by using $\bar{P}$ to denote the weighted sum of the neighborhood polarizations $\sum_i P_i f_i$. Using this Hamiltonian the steady state polarization is given by

$$P^{ss} = -\lambda_3^{ss} = \rho_{11}^{ss} - \rho_{00}^{ss} = \frac{E_k\bar{P}}{\sqrt{E_k^2\bar{P}^2 + 4\gamma^2}}\tanh\left(\frac{\sqrt{E_k^2\bar{P}^2/4+\gamma^2}}{kT}\right) \tag{4}$$

Eq. 4 can be written as

$$P^{ss} = \frac{E}{\Omega}\tanh(\Delta) \tag{5}$$

where $E = 0.5\sum_i E_k P_i f_i$, total kink energy and Rabi frequency $\Omega = \sqrt{E_k^2\bar{P}^2/4+\gamma^2}$ and $\Delta = \frac{\Omega}{kT}$ is the thermal ratio. We will use the above equation to arrive at the probabilities of observing (upon making a measurement) the system in each of the two states. Specifically, $\rho_{11}^{ss} = 0.5(1+P^{ss})$ and $\rho_{00}^{ss} = 0.5(1-P^{ss})$, where we made use of the fact that $\rho_{00}^{ss} + \rho_{11}^{ss} = 1$.

3 Approach

We propose a Bayesian Network based modeling and inference for the QCA cell polarization.

A Bayesian network[11] is a Directed Acyclic Graph (DAG) in which the nodes of the network represent random variables

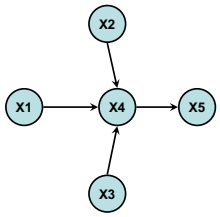

Figure 1: A small Bayesian network

and a set of directed links connect pairs of nodes. The links represent causal dependencies among the variables. Each node has a conditional probability table (CPT) except the root nodes. Each root node has a prior probability table. The CPT quantifies the effect the parents have on the node. Bayesian networks compute the joint probability distribution over all the variables in the network, based on the conditional probabilities and the observed evidence about a set of nodes.

Fig. 1 illustrates a small Bayesian network that is a subset of a Bayesian Network for a majority logic. In general, x_i denotes some value of the variable X_i and in the QCA context, each X_i is the random variable representing an event that the cell is at steady-state logic "1" or at steady state logic "0". The exact joint probability distribution over the variables in this network is given by Eq. 6.

$$\begin{aligned} P(x_5,x_4,x_3,x_2,x_1) &= P(x_5|x_4,x_3,x_2,x_1) \\ &\quad P(x_4|x_3,x_2,x_1)P(x_3|x_2,x_1) \\ &\quad P(x_2|x_1)P(x_1). \end{aligned} \tag{6}$$

In this BN, the random variable, X_5 is independent of X_1, given the state of its parents X_4 This *conditional independence* can be expressed by Eq. 7.

$$P(x_5|x_4,x_3,x_2,x_1) = P(x_5|x_4) \tag{7}$$

Mathematically, this is denoted as $I(X_5,\{X_4\},\{X_1,X_2,X_3\})$. In general, in a Bayesian network, given the parents of a node n, n and its descendents are independent of all other nodes in the network. Let U be the set of all random variables in a network. Using the conditional independencies in Eq. 7, we can arrive at the minimal factored representation shown in Eq. 8.

$$\begin{aligned} P(x_5,x_4,x_3,x_2,x_1) &= P(x_5|x_4)P(x_4|x_3,x_2,x_1) \\ &\quad P(x_3)P(x_2)P(x_1). \end{aligned} \tag{8}$$

In general, if x_i denotes some value of the variable X_i and $pa(x_i)$ denotes some set of values for X_i's parents, the minimal factored representation of exact joint probability distribution over m random variables can be expressed as in Eq. 9.

$$P(X) = \prod_{k=1}^{m} P(x_k|pa(x_k)) \tag{9}$$

Note that, Bayesian Networks are proven to be minimal representation that can model all the independencies in the

probabilistic model. Also, the graphical representation in Fig. 1 and probabilistic model match in terms of the conditional independencies. Since Bayesian Networks uses directional property it is directly related to inference under causality. In a clockless QCA circuit, cause and effect between cells are hard to determine as the cells will affect one another irrespective of the flow of polarization. Clocked QCA circuits however have innate ordering sense in them. Part of the ordering is imposed by the clocking zones. Cells in the previous clock zone are the drivers or the causes of the change in polarization of the current cell. Within each clocking zone, ordering is determined by the direction of propagation of the wave function [10].

Let $Ne(X)$ denote the set of all neighboring cells that can effect a cell, X. It consists of all cells within a pre-specified radius. Let $C(X)$ denote the clocking zone of cell X. We assume that we have phased clocking zones, as has been proposed for QCAs. Let $T(X)$ denote the time it takes for the wave function to propagate from the nodes nearest to the previous clock zone or from the inputs, if X shares the clock with the inputs. Note that only the relative values of $T(X)$ are important to decide upon the causal ordering of the cells. Thus, given a set of cells, we can exactly predict (dependent on the effective radius of influence assumed) the parents of every cell and all the non-parent neighbors. In this work, we assume to use *four* clock zones. We denote this parent set by $Pa(X)$. This parent set is logically specified as follows.

$$Pa(X) = \{Y | Y \in Ne(X), (C(Y) <_{mod4} C(X)) \vee (T(Y) < T(X))\} \quad (10)$$

The *causes*, and hence the parents, of X are the cells in the previous clocking zone and the cells are nearer to the previous clocking zone than X. The children set, $Ch(X)$, of a node, X, will be the neighbor nodes that are not parents, i.e. $Ch(X) = Ne(X)/Pa(X)$.

The next important part of a Bayesian network specification involves the conditional probabilities $P(x|pa(X))$, where $pa(X)$ represents the values taken on by the parent set, $Pa(X)$.

We choose the children states (or polarization) so as to maximize $\Omega = \sqrt{E_k^2 \bar{P}^2/4 + \gamma^2}$, which would minimize the ground state energy over all possible ground states of the cell. Thus, the chosen children states are

$$ch^*(X) = \arg\max_{ch(X)} \Omega = \arg\max_{ch(X)} \sum_{i \in (Pa(X) \cup Ch(X))} E_k \bar{P} \quad (11)$$

The steady state density matrix diagonal entries (Eq. 5 with these children state assignments are used to decide upon the conditional probabilities in the Bayesian network (BN).

$$\begin{aligned} P(X=0|pa(X)) &= \rho_{00}^{ss}(pa(X), ch^*(X)) \\ P(X=1|pa(X)) &= \rho_{11}^{ss}(pa(X), ch^*(X)) \end{aligned} \quad (12)$$

Once we compute all the conditional probabilities, we provide prior probabilities for the inputs. We can then infer the Bayesian Networks to obtain the steady state probability of observing all the cells including the outputs at "1" or "0".

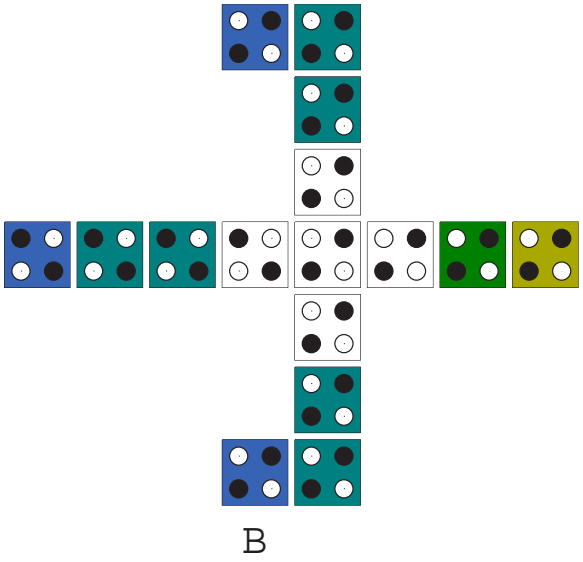

Figure 2: Clocked QCA majority gate layout

4 Experimental Results

In this section, we discuss the results of our model with a small example of three input majority gate as the cell layout of for QCA can be effectively drawn with synthesis using inverter and majority gates. Fig. 4 shows the cell layout of the majority gate. The Bayesian Network structure is shown in Fig 3. Note that we obtain the structure based on the causal flow of the wave function and the information regarding the clock zone. We use "Genie" [12] software tool for Bayesian inference. We present the extended view of the Bayesian Network shown in Fig. 4 with the polarization of each cell shown for a particular input set.

In Fig 5, we report the steady state probabilities of the correct outputs w.r.t temperature and we show that the probability of correct output vary with the input space. As we can see that the temperature plays a key role in obtaining correct signal behavior. More effect of temperature is less for some inputs say $\{0,1,1\}$ than $\{0,0,1\}$. Also, the input set $\{0,0,1\}$ and $\{0,1,0\}$ shows different sensitivity. Hence layout plays an important role in the error behavior of QCA. We validated our model with respect to the QCADesigner and received the same accuracy using the temporal simulation. However, the time for the simulation is an order of magnitude faster.

REFERENCES

[1] S. Bhanja and N. Ranganathan, "Switching activity estimation of vlsi circuits using bayesian networks," *IEEE Transactions on VLSI Systems*, pp. 558–567, February 2003.

[2] S. Bhanja and N. Ranganathan, "Cascaded bayesian inferencing for switching activity estimation with correlated inputs," *Accepted for publication in IEEE Transaction on VLSI*, 2004.

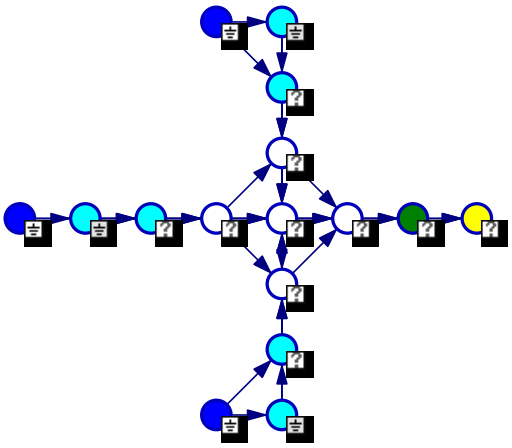

Figure 3: Bayesian net dependency structure corresponding to the QCA majority gate with nodes corresponding to the individual cells and links denoting direct dependencies.

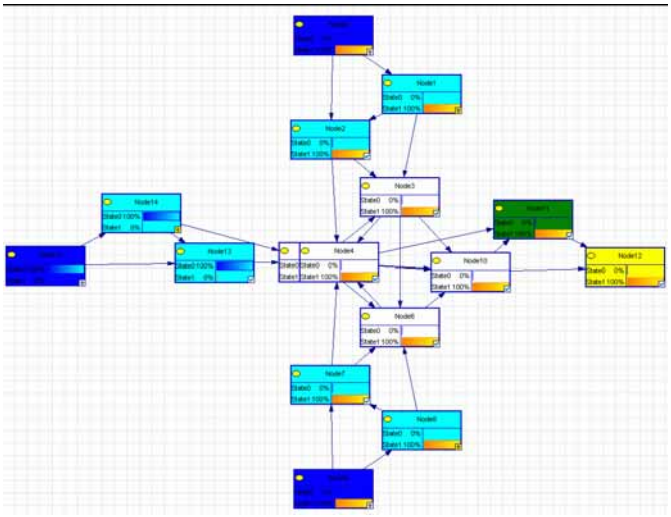

Figure 4: Exploded view of the Bayesian net structure, laying bare the directed link structure and the node information using ”Genie” [12].

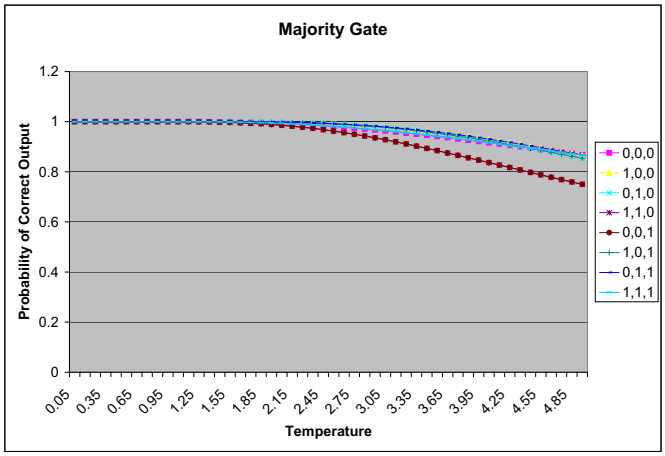

Figure 5: Dependence of probability of correct output of the majority gate with temperature *and* inputs. Note the dependence on inputs.

[3] C. Lent and P. Tougaw, “A device architecture for computing with quantum dots,” in *Proceeding of the IEEE*, vol. 85-4, pp. 541–557, April 1997.

[4] C. Lent and B. Isaken, “Clocked molecular quantum-dot cellular automata,” *IEEE Transactions on Electron Devices*, vol. 50, pp. 1890–1896, September 2003.

[5] G. Toth and C. Lent, “Role of correlation in the operation of quantum-dot cellular automata,” *Journal of Applied Physics*, vol. 89, pp. 7943–7953, June 2001.

[6] I. Amlani, A. Orlov, G. Snider, C. Lent, W. Porod, and G. Bernstein, “Experimental demonstration of electron switching in a quantum-dot cellular automata (qca) cell,” *Superlattices and Microstructures*, vol. 25, no. 1/2, pp. 273–278, 1999.

[7] K. Walus, T. Dysart, G. Jullien, and R. Budiman, “QCADesigner: A rapid design and simulation tool for quantum-dot cellular automata,” *IEEE Trans. on Nanotechnology*, vol. 3, pp. 26–29, March 2004.

[8] J. Timler and C. Lent, “Power gain and dissipation in quantum-dot cellular automata,” *Journal of Applied Physics*, vol. 91, pp. 823–831, January 2002.

[9] Y. Wang and M. Lieberman, “Thermodynamic behavior of molecular-scale quantum-dot cellular automata (QCA) wires and logic devices,” *IEEE Transactions on Nanotechnology*, vol. 3, pp. 368–376, Sept. 2004.

[10] P. Douglas Tougaw and C. S. Lent, “Dynamic behavior of quantum cellular automata,” *Journal of Applied Physics*, vol. 80, pp. 4722–4736, Oct 1996.

[11] J. Pearl, *Probabilistic Reasoning in Intelligent Systems: Network of Plausible Inference*. Morgan Kaufmann, 1988.

[12] `http://www.sis.pitt.edu/~genie`